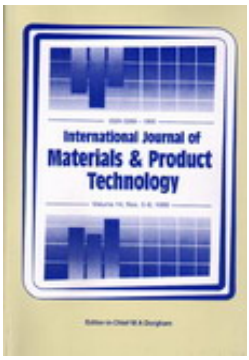

International Journal of Materials and Product Technology

ISSN online: 1741-5209 - ISSN print: 0268-1900
https://www.inderscience.com/ijmpt

Colour fixation process and colour fastness improvement strategies for natural plant dyes in functional clothing fabrics

Jiaheng Han, Zicheng Zhang, Jiang Chang

DOI: 10.1504/IJMPT.2026.10078276

Article History:

Received:	26 September 2025
Last revised:	17 March 2026
Accepted:	02 April 2026
Published online:	30 July 2026

Colour fixation process and colour fastness improvement strategies for natural plant dyes in functional clothing fabrics

Jiaheng Han

Department of Fashion Design,
Tangshan University,
Tangshan, 063000, Hebei, China
Email: 18401037@masu.edu.cn

Zicheng Zhang and Jiang Chang*

School of Design,
University of Leeds,
Leeds, LS2 9JT, England, UK
Email: 39006585@qq.com
Email: jchang0520211@163.com
*Corresponding author

Abstract: The application of natural plant dyes in functional textiles is limited by poor colour fastness and difficulty in colour fixation. Functional additives can reduce fibre surface polarity, shield active sites, and hinder dye uptake. Traditional metal mordant dyeing methods also carry the risk of chemical interference with functional components, compromising performance stability. This study proposes an optimised colour fixation method. First, plant dyes compatible with functional fabrics are selected, and dyeing parameters are adjusted to ensure uniform dye penetration into the fibres. Then, a customised fixing agent is used to enhance dye-fibre bonding through high-temperature steam and mild chemical crosslinking. Dyeing conditions (such as pH, time, and temperature) are further optimised to improve colour fixation. Results show that after 25 washes, the antibacterial fabric achieves a wash fastness of 2.7, with a dye residue rate of 70.1%. The light fastness remains at 3.9 (initial value: 5) after 120 hours of exposure, and the antibacterial rate remains at 91.6% after washing. This method effectively improves colour durability while preserving the fabric's functional properties.

Keywords: natural plant dyes; functional clothing fabrics; colour fixation process; colour fixing agent formulation; dyeing process.

Reference to this paper should be made as follows: Han, J., Zhang, Z. and Chang, J. (2026) 'Colour fixation process and colour fastness improvement strategies for natural plant dyes in functional clothing fabrics', *Int. J. Materials and Product Technology*, Vol. 70, No. 6, pp.3–26.

Biographical notes: Jiaheng Han obtained his Doctoral in Design Engineering from Gaya University, South Korea, and received his Master's in Design from Dalian Polytechnic University, China. He currently serves as a faculty member in the Department of Fashion Design at Tangshan College. His primary research areas include fashion design, traditional culture studies, textile materials science, and the integration of art and technology.

Zicheng Zhang received his Master's degree from the School of Visual Arts. Now, he studies in the School of Design, University of Leeds. His research interests include cultural heritage preservation, design, and artificial intelligence, with a focus on multi facet artistic practice.

Jiang Chang received his Bachelor's degree from Southampton University, and Master's degree from Central Saint Martins, University of the Arts London. He is currently studying for a PhD at the School of Design, University of Leeds. His research interests include the digitisation of intangible cultural heritage in the field of human-computer interaction, computer vision, etc.

1 Introduction

As environmental awareness increases, natural plant dyes have received considerable attention from the textile industry as dyeing materials, as they cause less environmental pollution and are more biodegradable than synthetic dyes. Furthermore, in some cases, natural plant dyes can give special colours and textures to products (Lin et al., 2022; Pizzicato et al., 2023). Therefore, the application of natural plant dyes in the fashion industry and in functional clothing fabrics has been gradually increasing (Che and Yang, 2022; Lai and Chang, 2021). Functional clothing fabrics have a wide range of applications in modern textiles due to their special properties, such as antibacterial, breathable, UV-resistant, and waterproof characteristics (Junior et al., 2022; Xiao and Kan, 2022). However, natural plant dyes have poor colour fastness, especially in dyeing functional fabrics. Traditional dyeing technology cannot improve dye adhesion and fastness, and it is limited in the production of high-performance functional fabrics (Otaviano et al., 2023; Wang et al., 2024). The poor colour fastness of natural plant dyes, including light, water, and friction fastness, makes dyed fabrics prone to fading, which affects the service life and appearance of clothing (Saeed et al., 2023; Turgut et al., 2023). Therefore, improving the colour fastness of natural plant dyes and preserving the original properties of functional fabrics are urgent technical problems for the textile industry (Harsito et al., 2021; Hannan et al., 2023).

Conventional methods to enhance colour fastness often involve metal mordants, which coordinate dye molecules to fibre substrates. These metal ions present environmental concerns in effluent treatment, as they resist degradation and accumulate in aquatic systems, necessitating costly removal processes before wastewater discharge. Beyond ecological impact, metal mordants may interact with functional finishes integrated into fabrics, potentially diminishing desired attributes such as antimicrobial efficacy or UV resistance through competitive binding or structural interference with active components. The pursuit of sustainable textile processing has thus motivated the exploration of alternative fixation strategies that avoid the use of heavy metals while ensuring robust dye-fibre binding. Biopolymer-based fixing agents, particularly those derived from chitosan, have attracted interest owing to their cationic properties, which facilitate electrostatic attraction to anionic dyes, offering a metal-free pathway for colour retention. Yet their deployment in functional fabrics necessitates careful parameter control to preserve the specialised properties imparted to the material, as excessive crosslinking or non-selective binding could alter surface characteristics or block functional sites. This background underscores the need for a fixation approach that can

enhance dye durability without compromising the fabric's functional integrity, integrating principles from both biopolymer chemistry and natural product interactions to achieve stable coloration while maintaining the advanced performance characteristics that define functional textiles.

Therefore, this study aims to develop an improved fixation method for natural plant dyes in functional textiles. Suitable dyes are selected based on the functional properties of the fabrics. Meanwhile, the dyeing temperature, time, and pH are optimised to achieve uniform dye uptake and good fibre fixation. An improved fixation system was designed using high-temperature steaming and mild chemical crosslinking. The system formed a non-covalent network composed of a quaternised chitosan derivative and ellagic acid. The dyes were fixed by electrostatic interaction and polyphenol hydrogen bond. The method was free of metal ions and did not interfere with the subsequent application of antimicrobial metal mordants, since these mordants often cause precipitation and lose their activity. Meanwhile, the fixing process improved the binding of natural plant dyes to fibre and preserved the activity of the functional additive in fibre. The amount and type of fixing agent were controlled to ensure that they did not affect the fabric's functional properties. The fastness of the dye was evaluated by washing, light, and abrasion. The results showed that the fixing process improved the binding of dyes to the fibre without damaging the activity of the functional additive. The improved method extended the use of natural dyes in functional textiles and offered a new approach to advanced sustainable dyeing technology.

2 Related work

Detailed research on the fixation of natural plant dyes in functional textiles encompasses a multidimensional academic framework. Thakker and Sun (2021) have reviewed the entire panorama of ancient biomaterial engineering and herbal colorants, with emphasis on the medicinal and ecological attributes of natural dyes, such as UV shielding, antibacterial activity, etc., and their contribution to the development of sustainable, slow-tech textiles. This work has been theoretically backed for studying multifunctionality of natural dyes (Wang et al., 2026; Salian et al., 2021) Ragab and Hassabo (2021) carried out a detailed investigation on application of plant extracts like peanut pods, olive leaves, etc. for dyeing cotton and wool with emphasis on their environmental friendly nature and zero waste burden which has supported revival of green dyeing technology at global level. These examples corroborate the environmentally friendly behaviour of natural dyes in practical applications (Sk et al., 2021; Alegbe and Uthman, 2024). Hossain et al. (2022) designed a cationic fixative/D5 microemulsion system in a non-aqueous, mordant-free medium and optimised process parameters using an L9 orthogonal test to enhance the colour yield, rubbing fastness, washing fastness, and UV shielding properties of cotton fabrics dyed with cocoa shell extract. This work establishes a new direction for green dyeing technology (Saleem et al., 2023; Bairabathina et al., 2022). However, the majority of current research on functional fabrics is scant in its in-depth study of the interaction behaviour of functional additives with the colour fastness of these fabrics.

Research on the colour fastness of natural plant dyes in functional clothing fabrics: exploration of diversified technical paths. Mandal and Venkatramani (2023) reviewed the research progress on natural dyes in leather dyeing over the last 20 years, examined their

environmental characteristics and colour fastness performance, and highlighted the need for a sustainable dyeing process. It provides an important theoretical basis for the study of colour fastness (Mao and Xu, 2024; Cruz et al., 2021). Talib et al. (2023) carried out microwave-assisted extraction of black pepper colorant and integrated response surface methodology to optimise the dyeing parameters, thereby enhancing the colour depth and colour fastness performance indicators of silk fabrics using bio-mordants. This approach has achieved a significant breakthrough in improving the colour fastness stability in silk dyeing (Aftab et al., 2025; Gala et al., 2022). Habib et al. (2021) employed ultrasound-assisted extraction of Arjun bark colourant and integrated bio-mordants to optimise the cotton fabric dyeing process. This method is useful for improving colour intensity and hue performance (Benli, 2024; Hosseinnezhad et al., 2022). Generally, the above results neglect the interactive mechanisms between functional additives and improvement strategies for colour fastness in functional clothing fabrics.

3 Fixation process optimisation methods

3.1 Plant dye screening and functional fabric compatibility evaluation

A quantitative analysis model was developed to evaluate the compatibility of plant dyes with functional fabrics by considering intermolecular interactions. Plant dye molecules interact with fibre surfaces via van der Waals interactions, hydrogen bonds, electrostatic attraction interactions, and π–π stacking. Different plant dye classes exhibit distinct binding behaviour, governed by their chemical composition and functional groups. The colour fastness of plant dyes depends on the binding strength and stability of the above interactions. To understand these interactions at the molecular level, it is essential to develop an effective fixation strategy that enhances dye-fibre interactions without damaging functional fabrics. The binding energy between the dye molecule and the fibre is determined using a quantum-chemical calculation method. The binding energy determines the adsorption energy of the dye on the fibre surface (Hussain et al., 2024; Ibrahim et al., 2024). The binding energy of the solute–fibre system was calculated by density functional theory (DFT), and the formula is shown.

$$E_{bind} = E_{dye-fiber} - \left(E_{dye} + E_{fiber}\right) \tag{1}$$

E_{bind} is the dye-fibre binding energy; $E_{dye\text{-}fibre}$ is the total energy of the dye molecule and the fibre fragment; E_{dye} is the energy of the isolated dye molecule; E_{fibre} is the energy of the isolated fibre fragment. The calculation process used the B3LYP functional and the 6-31G(d,p) basis set. The solvent effect was simulated with the polarisable continuum model (PCM) in water (Abdel-Kader et al., 2024; Aracena et al., 2024).

The characteristic parameters of the plant dye molecule are obtained by system characterisation. The molecular weight is determined by matrix-assisted laser desorption ionisation time-of-flight mass spectrometry. The polarity index is determined by the ratio of dipole moment to molecular volume, and the calculation formula is:

$$PI = \frac{\mu}{V_m} \tag{2}$$

PI is the polarity index; μ is the molecular dipole moment; V_m is the molecular volume. The molecular polarity index is calculated using water as the solvent to reflect dye behaviour during textile processing accurately. This aqueous environment affects the dipole moments by hydrogen bonding with polar functional groups on the plant dye molecules. Polarisation index values obtained via this water-based simulation reflect the actual interaction properties of the dye-fibre in practical dye bath systems rather than theoretical gas-phase properties. This selection of solvent environment guarantees the validity of the molecular characteristic parameters with respect to real textile application conditions.

Zeta potential was measured by the Zetasizer Nano ZS instrument (Malvern instruments). The average value was calculated by repeating the same sample 10 times. Solubility was measured by UV – visible spectrophotometry (Lepre et al., 2021; Hossain, 2023).

Table 1 Molecular characteristic parameters of plant dyes

Dye name	*Molecular weight range* (*g/mol*)	*Polarity index* ($D{\cdot}Å^{-3}$)	*Zeta potential* (*mV*)	*Solubility* (*mg/mL*)
Turmeric	368.12–368.37	1.78	–24.5	0.85
Indigo	262.27–262.42	2.15	–31.2	0.63
Rubia cordifolia	254.24–254.39	1.96	–28.7	0.72
Gardenia	408.36–408.51	1.65	–22.3	0.91
Sumu	286.24–286.39	2.03	–29.8	0.68
Lithospermum officinale	288.25–288.40	1.82	–25.6	0.76
Cochineal	492.41–492.56	1.54	–20.9	0.52
Tea	458.34–458.49	2.27	–33.4	0.59
Mulberries	464.38–464.53	2.39	–35.1	0.48
Black beans	590.52–590.67	1.42	–18.7	0.64
Gardenia yellow	408.36–408.51	1.65	–22.3	0.91
Gallnut	1,700.85–1701.00	0.87	–15.2	0.37

Table 1 shows the basic parameters of molecular characteristics of 12 plant dyes in a systematic way, such as the molecular weight range, polarity index, Zeta potential, and solubility data under normal conditions, which represent the physical and chemical properties of the molecules of dye and provide a quantitative basis for the evaluation of the compatibility of dyes and functional fabrics.

Characteristic parameters of the surface of functional fabrics. Surface energy, porosity, and contact angle are the three basic parameters of surface characteristics of functional fabrics. Owens-Wendt calculates surface energy.

$$\gamma_s(1+\cos\theta) = 2\left(\sqrt{\gamma_s^d \gamma_l^d} + \sqrt{\gamma_s^p \gamma_l^p}\right) \tag{3}$$

γ_s is the solid surface energy; θ is the contact angle; γ_s^d and γ_s^p are the dispersion component and polar component of the solid surface energy, respectively; γ_l^d and γ_l^p are the corresponding components of the liquid. The calculation of dispersed and polar components follows the Owens-Wendt method using two standard liquids.

The system of equations is expressed as: $\cos\theta_1 + 1 = 2\frac{\sqrt{\gamma_s^d \gamma_{l1}^d} + \sqrt{\gamma_s^p \gamma_{l1}^p}}{\sqrt{\gamma_s^d + \gamma_s^p} + \sqrt{\gamma_{l1}^d \gamma_{l1}^p}}$, $\cos\theta_2 + 1 = 2\frac{\sqrt{\gamma_s^d \gamma_{l2}^d} + \sqrt{\gamma_s^p \gamma_{l2}^p}}{\sqrt{\gamma_s^d + \gamma_s^p} + \sqrt{\gamma_{l2}^d + \gamma_{l2}^p}}$. Where water $\left(\gamma_{l1}^d = 21.8\ mJ/m^2,\ \gamma_{l1}^p = 51.0\ mJ/m^2\right)$ and diiodomethane $\left(\gamma_{l2}^d = 50.8\ mJ/m^2, \gamma_{l2}^d = 0\ mJ/m^2\right)$ serve as standard test liquids. Verification is achieved through 10 repeat measurements at various locations on the fabric, with a relative standard deviation < 5%, and comparison with polytetrafluoroethylene reference samples ensures the accuracy of the measured value.

In the test, there are two standard liquids: deionised water (polar) and diiodomethane (non-polar). Each liquid is measured 10 times at various locations on the fabric. Surface roughness was measured using atomic force microscopy (AFM). Porosity was measured using mercury intrusion. Surface roughness directly affects the contact area between the dye molecule and the fibre surface, thereby influencing adsorption capacity and stability. The effective contact area A equals A0 multiplied by one plus k times Ra. The adsorption energy Ead equals negative kB times T times natural logarithm of one plus alpha times Ra. Higher surface roughness increases the effective contact area but may cause uneven dye distribution. The optimal Ra value for functional fabrics ranges from fifteen to thirty nanometers. Molecular dynamics simulations confirm that Ra values exceeding 35 nanometers lead to unstable adsorption configurations, while values below ten nanometers reduce dye retention significantly.

Table 2 Surface characteristic parameters of three types of functional fabrics

Fabric type	*Surface energy* (mJ/m^{-2})	*Porosity* (%)	*Water contact angle* (°)	*Surface roughness* R_a (nm)	*Average pore size* (μm)
-	Total value	Dispersed components	Polarity component	-	Water
Antibacterial	42.7	35.2	7.5	28.5 ± 1.2	118.3
UV-resistant type	38.4	31.6	6.8	23.7 ± 0.9	132.6
Waterproof and breathable	29.5	26.3	3.2	19.2 ± 0.7	147.8

Table 2 presents the surface characteristic parameters of three types of functional fabrics: antibacterial, anti-ultraviolet, and waterproof and breathable, including surface energy component, porosity, two-liquid contact angle, Ra, and average pore size, which accurately characterise the physical and chemical properties of the fabric surface and support the study of the dye-fibre interaction mechanism.

The chemical composition of the fabric is analysed by x-ray photoelectron spectroscopy (XPS), and the spectrum is analysed using advantage software for peak fitting and quantitative element analysis. The interaction mechanism between the dye molecules and the fibre surface is verified by molecular dynamics simulation to ensure that the system reaches an energy balance state.

The adaptability evaluation adopts a multi-parameter weighted scoring model, and the calculation formula is:

$$S = \alpha \frac{E_{bind}}{E_{max}} + \beta \frac{|\Delta PI|}{PI_{max}} + \gamma \frac{|\Delta Z|}{Z_{max}} \tag{4}$$

S is the adaptability score (dimensionless); α, β and γ are weight coefficients; E_{max} is the maximum binding energy reference value; ΔPI is the difference between polarity index of dye and fibre; PI_{max} is the maximum reference value of polarity index; ΔZ is the difference between Zeta potential of dye and fibre; Z_{max} is the maximum reference value of Zeta potential. The model estimates each parameter weight using a hierarchical analysis method, ensuring that the evaluation results reflect the actual adaptability of the dye and the functional fabric.

The polarity index of plant dye molecules shows a clear, decisive correlation with the surface energy parameters of functional fabrics. It influences the extent of dye adsorption via intermolecular interactions. The ratio of the polarity index difference to the polar component of surface energy is a key quantitative indicator that directly determines the dye–fibre binding energy. The relative proportion of polar to dispersive components of surface energy influences the molecular arrangement configuration and adsorption orientation of plant dye molecules on the fibre surface. The plant dye molecules' adsorption on the fibre surface, particularly on the polar component surface, can form a dense adsorption layer via hydrogen bonding and dipole–dipole interactions, thereby enhancing adsorption stability.

3.2 Fixing agent formulation design and chemical crosslinking mechanism

Based on a study of interactions between the dye and fibre, a dual-functional, synergistic fixative formulation is designed using a quaternised chitosan derivative and ellagic acid. The concentration range, molecular properties, and functional parameters of each component in the fixing agent are listed in Table 3. Chemical name of each component: main fixative component: quaternised chitosan derivative; crosslinking enhancer: ellagic acid; pH adjuster: sodium citrate; stabiliser: polyvinyl pyrrolidone.

Table 3 Fixing agent formulation composition parameters

Component type	*Concentration range (g/L)*	*Molecular characteristics*	*Functional parameters*
Main colour fixative ingredient	3.5–4.0	Quaternary ammonium group content 92.3±1.5%	2.15 ± 0.08 meq/g
Cross-linking enhancer	1.8–2.2	8 phenolic hydroxyl groups	0.87 ± 0.03 (dimensionless)
pH adjusters	0.8–1.2	Sodium tricarboxylate	0.45 ± 0.02 mol·pH^{-1}·L^{-1}
Stabiliser	0.5–0.8	Molecular weight 40,000 g/mol	0.12 ± 0.01 g/L

The concentration range of the quaternised chitosan derivative is determined based on a comprehensive study of electrostatic interaction energies and adsorption equilibria. A thermodynamic calculation based on the Poisson-Boltzmann equation relates the concentration of the quaternary ammonium group to the dye-fibre binding energy. The fixing agent was prepared with seven concentration gradients ranging from 3.0 to 4.5 g/L in 0.25 g/L intervals. The corresponding water fastness, light fastness, and the retention

of functional property after 25 washes were determined. The results indicated that dye loss would be significant when the concentration was below 3.5 g/L due to insufficient electrostatic bonding. A concentration range of 4.0 to 4.5 g/L would result in a high crosslinking density, low fabric flexibility, and retention of functional properties. The optimal concentration range of 3.5–4.0 g/L could get the maximum binding energy of 14.2 kJ/mol without damaging the fabric property. The quantitative relationship between the amount of quaternised chitosan derivative and the surface energy parameters of functional fabrics was established by linking the adsorption free energy calculated from surface energy components to the optimal fixing agent concentration. For antibacterial fabric with high surface energy, the computed maximum adsorption free energy corresponded to the optimal concentration range of 3.5–4.0 g/L. For a waterproof and breathable fabric with low surface energy, the lower adsorption-free energy necessitated a reduced fixing agent concentration. This relationship elucidates the dosage adaptability across different functional fabrics and provides a theoretical basis for process optimisation. This range maintained charge density at 2.15 ± 0.08 meq/g ensuring effective electrostatic adsorption without compromising fibre structural integrity.

The following formula calculates the electrostatic interaction energy between the chitosan derivative and the dye molecule:

$$E_{elec} = \frac{q_1 q_2}{4\pi\varepsilon_0\varepsilon_r r'} \tag{5}$$

E_{elec} represents the electrostatic interaction energy; q_1 is the charge of the quaternary ammonium group of the chitosan derivative; q_2 is the charge of the plant dye molecule; ε_0 is the vacuum dielectric constant; ε_r is the relative dielectric constant in water; r' is the distance between the two charge centres.

The strength of the hydrogen bond between ellagic acid and dye molecules is determined by equation (6):

$$E_{hb} = A\exp(-Br) - \frac{C}{r^6} \tag{6}$$

E_{hb} represents the hydrogen bond formation energy; A is the hydrogen bond strength coefficient; B is the decay constant; C is the van der Waals constant; and r is the distance between the hydrogen bond donor and the acceptor.

The crosslinked network structure formed by quaternised chitosan derivatives and ellagic acid within the fibre exhibits an intermolecular distance of 0.32 ± 0.03 nm. The electrostatic interaction energy distribution ranges from 12.5 to 14.8 kJ/mol, while the hydrogen bond formation energy distribution ranges from 8.7 to 10.2 kJ/mol. These parameter distributions ensure structural stability and uniform distribution of the crosslinked network within the fibre.

The change in Gibbs free energy verifies the thermodynamic feasibility of the crosslinking reaction:

$$\Delta G = \Delta H - T\Delta S \tag{7}$$

ΔG represents the change in Gibbs free energy; ΔH is the enthalpy change; T is the absolute temperature; and ΔS is the entropy change.

The penetration behaviour of the fixing agent in functional fabrics follows Fick's second law:

$$\frac{\partial C'}{\partial t} = D\frac{\partial^2 C'}{\partial x^2} \tag{8}$$

C' represents the fixing agent concentration; t is the time; D is the diffusion coefficient; x is the penetration depth. Figure 1 shows the chemical crosslinking reaction path of the dye-fixing agent-fibre ternary system.

Figure 1 Chemical crosslinking reaction of the dye-fixing agent-fibre ternary system (see online version for colours)

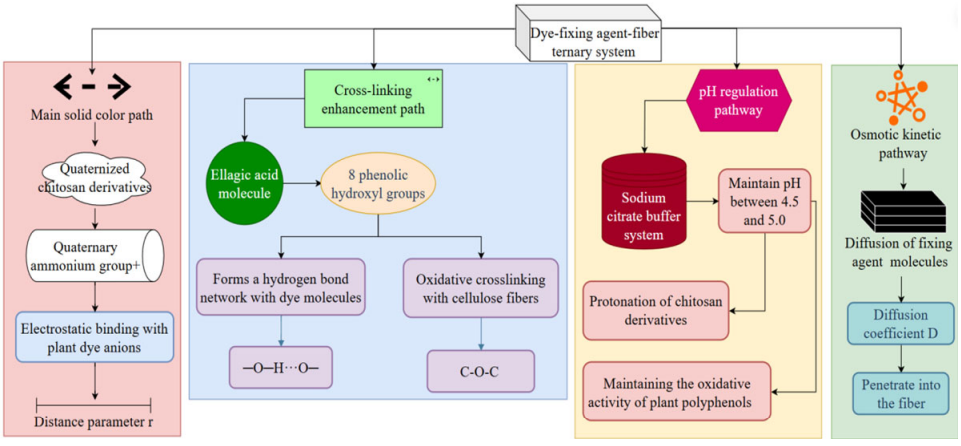

As shown in Figure 1, along the main fixing path, the quaternary ammonium group of the quaternised chitosan derivative forms an electrostatic bond with the plant dye anion within a distance r. In the cross-linking enhancement pathway, ellagic acid molecules simultaneously form hydrogen bonds with dye molecules through their eight phenolic hydroxyl groups and undergo oxidative cross-linking with cellulose fibres, forming C-O-C bonds. The pH control pathway shows that the sodium citrate buffer system stabilises the reaction environment in the pH range of 4.5–5.0. The permeation kinetic pathway shows that the fixing agent molecules penetrate the fibre interior with a diffusion coefficient D, forming a stable molecular-scale network.

The polarity index of plant dye molecules, a measure of dipole moment and hydrogen bonding propensity, governs the magnitude of electrostatic interactions with quaternised chitosan derivatives and the strength of hydrogen bonds with ellagic acid. Higher polarity indices intensify these interactions, promoting robust ternary network formation and superior colour fastness. Lower polarity indices reduce direct binding of the dye-fixing agent, making the crosslinked network more critical for dye retention. Thus, the polarity index difference directly influences the relative contributions of electrostatic and hydrogen bonding mechanisms to overall colour fixation.

3.3 Dynamic ph gradient control of dyeing process

Dynamic pH gradient control is based on the interaction between the ionisation state of dye molecules and the fibre surface charge. The formula for the ionisation degree α' of dye molecules is as follows:

$$\alpha' = \frac{1}{1+10^{pH-pK_a}} \tag{9}$$

pH is the pH of the solution, and pK_a is the characteristic dissociation constant of the dye. The degree of ionisation of the dye molecules exhibits a deterministic functional relationship with the surface charge density of the fibres during the dynamic process of controlling the pH gradient. With changes in pH, the ionisation degree exhibits an S-shaped curve and shows a nonlinear relationship with the fibre surface charge density. When pH is below the characteristic dissociation constant, the degree of ionisation is low, and the interaction with the fibre surface is weak. When pH is close to the characteristic dissociation constant, the degree of ionisation increases rapidly, and the interaction intensity with the fibre surface reaches a maximum. When pH is larger than the characteristic dissociation constant, the degree of ionisation is saturated, and the interaction intensity with the fibre surface will not increase significantly. Then, the adsorption kinetics of dyes and the efficiency of fixing colour on the fibre surface are controlled.

The isoelectric point pI is used as the basis for determining the initial pH value:

$$pI = \frac{pK_{a1} + pK_{a2}}{2} \tag{10}$$

pK_{a1} and pK_{a2} are the characteristic dissociation constants in the process of zwitterion formation of dye molecules. The pH gradient change during the dyeing process adopts an exponential decay model:

$$pH(t) = pH_{final} - \left(pH_{final} - pH_{initial}\right) \cdot e^{-kt} \tag{11}$$

$pH(t)$ represents the pH value at time t; $pH_{initial}$ is the initial pH value; pH_{final} is the target pH value; k is the decay coefficient; and t is the dyeing time. The decay coefficient k is obtained by evaluating pH behaviour and the dye molecule's ionisation state in an orderly manner. A nonlinear dynamics model builds a relationship between pH change and time. Validation data from different initial pH levels in the dyeing process are used to validate the method. Decay coefficient k ranges from 0.025 to 0.035 to realise the best uniformity of dye adsorption and colour fastness.

The pH control system adopts an adaptive fuzzy proportional-integral-derivative (PID) algorithm:

$$u(t) = K_p(t) \cdot e(t) + K_i(t) \cdot \int_0^t e(\tau)d\tau + K_d(t) \cdot \frac{de(t)}{dt} \tag{12}$$

$u(t)$ represents the control output signal; $K_p(t)$, $K_i(t)$, and $K_d(t)$ are time-varying PID coefficients; $e(t)$ is the deviation between the set pH value and the actual measured value.

3.4 Optimisation of high-temperature steam fixation parameters

The temperature, pressure, and time parameters of the high-temperature steam fixation process have a decisive effect on the binding state of the dye molecule and the fibre. A three-factor, three-level orthogonal experiment is carried out. The temperature level is

110°C, 120°C and 130°C; the pressure level is 0.15 MPa, 0.20 MPa and 0.25 MPa; the time level is 20 min, 30 min and 40 min.

The dye molecule's diffusion behaviour in the fibre is non-steady-state diffusion. The Arrhenius equation can be expressed in terms of temperature.

$$D = D_0 exp\left(-\frac{E_a}{RT}\right) \tag{13}$$

D is the diffusion coefficient of the dye in the fibre; D_0 is the pre-exponential factor; E_a is the apparent activation energy; R is the ideal gas constant; T is the absolute temperature. Increasing the temperature can increase the diffusion rate of dye molecules, but too high a temperature may cause them to degrade.

The influence of high-temperature steam on the fibre crystalline region structure has been revealed through thermal and moisture interactions. Thermal analysis has revealed that 120°C is the temperature at which diffusion kinetics and molecular stability are balanced; at lower temperatures, diffusion rates are not sufficient for complete fibre penetration, and at higher temperatures, the thermal degradation rate exceeds the binding rate. Activation energy of dye diffusion in cellulose fibre is 42.7 kJ/mol, and the threshold for molecular degradation is at 85.3 kJ/mol. At 120°C, the diffusion coefficient is 1.85×10^{-10} m^2/s, indicating that at this temperature the diffusion rate is sufficient for complete fibre penetration within 30 minutes, without exceeding the molecular degradation rate. The structural change in the fibre allows the integrity of the dye molecule to be maintained at 120°C and to achieve the maximum fibre binding. This way, the thermal degradation of the delicate chromophore is avoided, as it starts to decompose at temperatures over 125°C. Changes in the crystallinity index and the amorphous/crystalline ratio alter the diffusion path of dyes, and changes in the integrity of the crystalline structure hinder dye penetration and the availability of binding sites, which, in turn, affect the stability of dye binding in the fibre matrix.

The diffusion coefficient of the dye molecules shows time-dependent behaviour during the dyeing process. During the fibre emergence phase, the diffusion coefficient reaches its maximum value due to the concentration gradient between the dye bath and the fibre centre. The first diffusion phase of the fibre upon entry into the dye bath is a power-law function of time. The diffusion coefficient decreases over time during the dye-uptake process as the fibre approaches saturation. The time-dependent diffusion coefficient is mathematically expressed as $D(t) = D_0'(1–e^{–kt})$, where D_0' denotes the initial diffusion coefficient, and k represents a decay constant specific to the dye-fibre system. This temporal evolution of the diffusion coefficient directly impacts the uniformity of dye distribution within the fibre structure. Effective process optimisation requires consideration of this time-dependent diffusion behaviour to ensure consistent colour depth and fastness.

The quantitative relationship between vapour pressure and temperature is expressed by the modified Clausius-Clapeyron equation:

$$ln\left(\frac{P_2}{P_1}\right) = -\frac{\Delta H_{vap}}{R}\left(\frac{1}{T_2} - \frac{1}{T_1}\right) \tag{14}$$

P_1 and P_2 are the saturated vapour pressures at temperatures T_1 and T_2, respectively, and ΔH_{vap} is the enthalpy of vapourisation. This equation allows precise control of the vapour pressure to maintain saturation at a given temperature, preventing overheating.

A one-dimensional heat conduction model is used to study the effect of temperature gradient on dye fixation:

$$\frac{\partial T}{\partial t} = \alpha_1 \frac{\partial^2 T}{\partial x^2} \tag{15}$$

In equation (15), T' is the temperature distribution; t is the time; x is the coordinate in the fibre thickness direction; and α_1 is the thermal diffusivity. This model is used to optimise the heating rate, ensure uniform temperature distribution, and prevent uneven dye distribution caused by temperature gradient.

A distributed thermocouple array monitors the temperature uniformity, and the root mean square error (RMSE) is used to evaluate the temperature field uniformity:

$$RMSE = \sqrt{\frac{1}{n}\sum_{i=1}^{n}\left(T_i - \overline{T}\right)^2} \tag{16}$$

T_i is the temperature of the i^{th} measuring point; $\overline{T}$ is the average temperature; n is the total number of measuring points. The system is equipped with 12 evenly distributed K-type thermocouples to monitor and feed back the heating element power in real-time. The steam distribution uses a multi-hole injection system to ensure even distribution in the processing chamber, preventing local overheating or insufficient steam.

In large-scale industrial production, temperature uniformity control is reinforced by deploying additional sensors and optimising steam injection layouts to ensure a stable thermal field within the processing chamber. Real-time feedback control algorithms dynamically adjust heating power to compensate for thermal inhomogeneities arising from increased scale, thereby preserving consistent dye fixation performance.

3.5 Construction of multi-parameter coupling process model

The multi-parameter coupling process model takes the above-mentioned variables of dyeing temperature, pH value, time, and fixing agent concentration as the basic variables of the complete process optimisation system of dyeing. Based on the response surface method, a quantitative relationship model between process parameters and the colour fastness index is established, and the central composite design method is used to determine the distribution of experimental points. Model input variables: dyeing temperature, dynamic pH value, dyeing time, and fixing agent concentration; output variable: comprehensive colour fastness index. The expression of its mathematical model is shown in.

$$Y = \beta_0 + \sum_{i=1}^{4}\beta_i x_i + \sum_{i=1}^{4}\sum_{j\geq i}^{4}\beta_{ij} x_i x_j + \sum_{i=1}^{4}\beta_{ii} x_i^2 + \varepsilon \tag{17)}$$

β_0 is the constant term; β_i is the linear coefficient; β_{ij} is the interaction coefficient; β_{ii} is the quadratic term coefficient; x_i is the coded process parameter; ε is the random error term.

pH and temperature parameters interact nonlinearly with colour fastness, and this interaction is due to conformational changes in the molecular structure. The increase in temperature changes the equilibrium degree of dye ionisation; however, pH determines

the degree of ionisation. This interaction alters the electrostatic interaction strength between the dye anions and the quaternised chitosan derivatives. The two parameters interact synergistically; the optimal temperature range changes with pH. The change in the Gibbs free energy is affected by both parameters. This interaction results in a saddle-shaped response surface, with colour fastness peaking at certain pH-temperature combinations.

The sensitivity range of process parameters is determined via a global sensitivity analysis, and the Sobol indices are used to quantify each parameter's contribution to the output variable.

$$S_i = \frac{D_{X_i}\left(E_{X_{-i}}\left(Y \mid X_i\right)\right)}{D(Y)} \tag{18}$$

S_i is the first-order Sobol index of the i^{th} parameter; D_{X_i} represents the variance about X_i; $E_{X_{-i}}$ represents the expected value of other parameters except X_i; $D(Y)$ is the total variance of the output variable. This index reflects the degree of independent influence of a single parameter change on the output result. The parameter ranges and the dynamic response characteristics of the dyeing system determine step sizes for the Sobol index calculation. The pH value step size of 0.2 is chosen to reflect ionisation-state transitions while maintaining computational efficiency precisely.

Critical control point identification is based on parameter tolerance analysis to determine the acceptable fluctuation range of each process parameter. The parameter tolerance δ_i is:

$$\delta_i = \frac{\Delta Y_{max}}{\left|\frac{\partial Y}{\partial x_i}\right|_{x_i = x_{i,opt}}} \tag{19}$$

ΔY_{max} is the maximum acceptable drop in colour fastness; $\frac{\partial Y}{\partial x_i}$ is the partial derivative of the output variable with respect to the i^{th} parameter; $x_{i,opt}$ is the optimal value of the parameter. By determining the allowable deviation range for each parameter from its optimal value, process stability is ensured.

Model validation uses the k-fold cross-validation method to evaluate prediction accuracy, and RMSE quantifies the cross-validation error:

$$RMSE_{CV} = \sqrt{\frac{1}{n}\sum_{i=1}^{n}\left(Y_i - \hat{Y}_{i,-k}\right)^2} \tag{20}$$

n is the number of validation set samples; Y_i is the actual measurement value; $\hat{Y}_{i,-k}$ is the model prediction value excluding the k-fold data training. An RMSE value below 0.15 indicates that the model has good predictive ability and meets process control requirements.

Least-squares estimates model parameters, and the variance inflation factor (VIF) is used to assess multicollinearity. A VIF value lower than 5 indicates that the correlation

between parameters is within an acceptable range. Figure 2 shows the complete technical path from parameter input to optimisation results.

Figure 2 Multi-parameter coupling process parameter optimisation (see online version for colours)

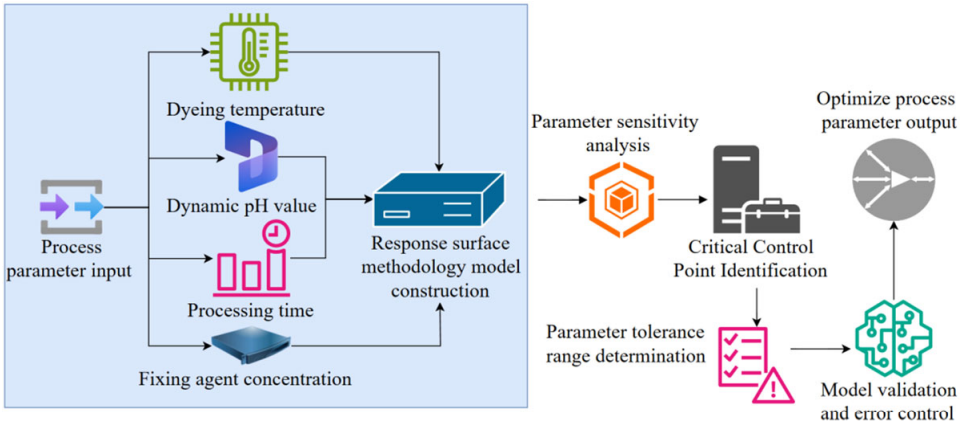

As shown in Figure 2, dyeing temperature, dynamic pH value, treatment time, and fixing agent concentration are integrated into a unified mathematical framework for collaborative optimisation, thereby avoiding the local-optimal solution problem associated with traditional single-factor optimisation methods. The parameter sensitivity analysis process in the above procedure is connected with the calculation of the Sobol indices. It can be used to determineto determine the contribution of the process parameters and provide a theoretical basis for optimal control parameters. The parameter tolerance range process determination takes the robust design idea into account, ensuring that the colour fastness indicator meets the quality requirement under actual production fluctuations.

4 Experimental design and validation

4.1 Experimental materials and test methods

The natural plant dyes used in this study are turmeric, indigo, and madder. These dyes have good colour and environmental performance in textile dyeing. All the dye samples used in the study are prepared from fresh plant materials. These materials are washed, dried, and pulverised by agricultural cooperatives. These plant materials are distilled to obtain a uniform dye material and a certain amount of dye. The extraction process is carried out for two hours at 80℃ under controlled conditions to obtain good dye absorption.

Antibacterial, UV-resistant, waterproof, and breathable are three functional fabrics chosen for the dyeing experiments. All fabrics are pretreated according to standard procedures before dyeing, such as soil removal, degreasing, and solid treatment, to ensure equal dye absorption.

Dyeing is controlled by adjusting temperature, time, and pH. The dye is fixed with a fixing agent. The fixing agent used in the study is prepared with quaternised chitosan

derivative and ellagic acid. The fixing agent provides a non-metallic crosslinking on the dye fabric. So it unifies the colour by increasing the dye attachment power.

The colour fastness of dyed fabrics is assessed by water fastness, light fastness, and abrasion fastness. Water fastness testing according to standard ISO 105-E01, the samples are immersed in deionised water for 24 hours. The choice to use the ISO 105-E01 standard for water-fastness evaluation is due to its well-established method for assessing the degree of colourant fading in textile materials when exposed to aqueous environments. This standard provides a well-established quantitative protocol for characterising the leaching behaviour of dyes in functional fabrics. Applicability verification for antibacterial fabrics testing was achieved by comparing with alternative standards that are consistent across different fabric types. The test parameters in this standard have been shown to agree with the properties of hydrophilic functional textile substrates. Hence, the parameters reflect real washing conditions. The lightfastness of the dyed fabrics is tested according to ISO 105-B02 with different light intensities. The abrasion resistance of the dyed fabrics is tested according to ISO 105-X12, under both dry and wet conditions.

The distribution of dye molecules within the fibre was characterised using AFM and laser confocal scanning microscopy. AFM was employed to observe the surface morphology of dyed fibres and the uniformity of dye coverage. Laser confocal scanning microscopy combined with cryosectioning was used to examine the cross-sectional distribution of dye molecules and their penetration depth within the fibre interior.

4.2 Experimental process and quality control

The experimental process begins with dye extraction and fabric pretreatment. Dyes are extracted by the distillation method to obtain a stable concentration. The pretreatment processes for the three types of functional fabrics include decontamination and degreasing to prepare for dyeing.

The dyeing process controls temperature, time, and pH to ensure uniform dye absorption and migration within the fibre. The fixing agent enhances the fixation of dyes onto fabrics during the dyeing process. The concentration and penetration of the fixing agent are strictly controlled to form a stable network of molecules.

Quality control is implemented in the whole experimental process. The concentration of the dye solution, temperature, and pH are monitored in the real-time monitoring system. The uniformity of temperature is monitored in the temperature control system to prevent uneven dye absorption caused by temperature differences. The pH is adjusted in real-time to improve the dye's ionisation and the fibre's binding.

Table 4 shows the quality control points used in the experiment. The quality control points are the dye solution concentration, temperature, pH, and fixing agent concentration.

In Table 4, the dye liquor concentration was monitored every hour using UV-V is spectrophotometry to maintain stability and compensate for concentration variations during the dyeing process. Temperature was measured every minute with a thermocouple to maintain uniformity during the dyeing process and prevent uneven dyeing caused by temperature variation. pH was measured in real-time with a pH meter and recorded every 15 min to maintain the dye's ionisation state within the desired range. The reason for recording pH values every 15 min is that this is the characteristic time scale for the dye ionisation phase transition. Molecular dynamics simulations demonstrated that changes in

the dye molecule's charge state occur at 12–15 minute intervals under standard conditions. Therefore, this time interval allows detection of the critical pH transitions that affect the electrostatic binding of the quaternised chitosan derivatives to the dye anions before they occur. Statistical process control methods were then applied, and the chosen monitoring interval was justified by its correlation with the colour fastness results, thus confirming the binding stability within the required specifications. The concentration of the fixing agent and its vapour pressure were measured for each batch to maintain the chemical and physical processes during fixation, according to predetermined conditions, thereby ensuring the process and optimal fixing results. These control measures maintain a high precision and reproducibility of the experiment and obtain optimal dye-fabric bonding.

Table 4 Distribution of quality control points and monitoring frequency

Control point name	*Monitoring methods*	*Monitoring frequency*
Dye concentration	UV-visible spectrophotometry	Per hour
Temperature	Thermocouple sensor monitoring	Per minute
pH	pH meter measurement	Every 15 minutes
Fixing agent concentration	Titration	Each batch
Steam pressure	Pressure sensor monitoring	Each batch

5 Results

5.1 Water fastness

Following the optimised fixation process, AFM imaging revealed a continuous, uniform dye layer on the fibre surface, with no significant alteration to the original surface morphology. Laser confocal scanning microscopy of fibre cross-sections demonstrated that dye molecules penetrated the fibre interior and were homogeneously distributed within a depth of approximately 10 micrometers from the surface. No evidence of dye aggregation or uncoloured regions was observed across the fibre cross-section, indicating effective and uniform dye penetration and fixation.

In addition to the above, to reveal the mechanism by which the optimised colour fixation process affects the water resistance of functional fabrics, the colour fastness of three types of functional fabrics is studied in detail in the present work during washing. Antibacterial fabrics with high surface energy and a moderate pore structure can provide favourable conditions for dye adsorption. UV-resistant fabrics have high water contact angles but low surface polarity, which makes it difficult for dye molecules to penetrate and fix. Waterproof and breathable fabrics have the lowest surface energy and strong hydrophilicity, so the interaction between the dye molecule and fibre is weakest. Colour fastness grades are evaluation indices of a fabric's ability to retain colour after washing, specified by the International Organisation for Standardisation (ISO 105-E01). Dye retention is a parameter that can accurately reflect the stability of the dye molecule in the fibre through quantitative analysis. Both of these parameters constitute the parameter system for evaluating colour fastness.

Figure 3 Evolution of water fastness performance of three types of functional fabrics (see online version for colours)

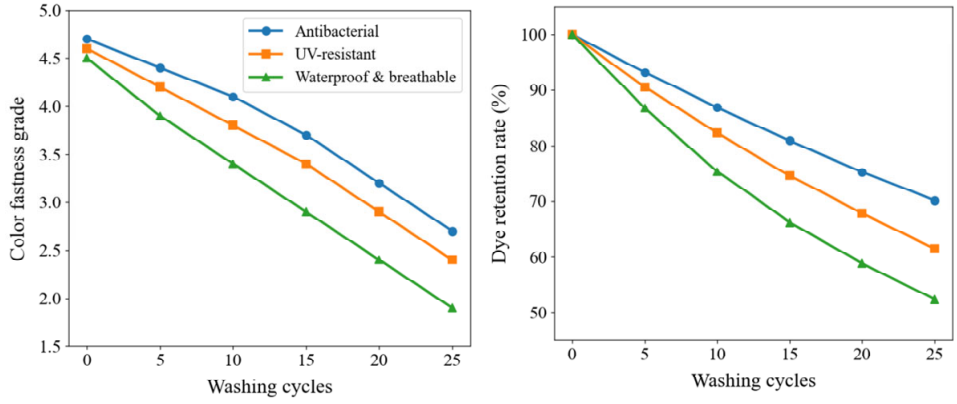

As shown in Figure 3, the dye grade of the three types of fabric is all above grade 4.5, meeting the requirements for colouring functional fabrics with natural plant dyes. After 25 washes, the antibacterial fabric still maintains grade 2.7; however, the UV-resistant fabric decreases to grade 2.4, and the waterproof/breathable fabric maintains only grade 1.9. The trend in dye retention closely matches the colour fastness grades. The antibacterial fabric can adsorb 70.1% of the dye after 25 washes; however, the waterproof/breathable fabric can only adsorb 52.3% of the dye after 25 washes. The above results are attributed to the interaction between the fibre's surface energy and the dye molecule. The higher surface energy of the antibacterial fabric enhances the electrostatic adsorption between the quaternised chitosan derivative and the dye anion. The orderly structure of the dispersed and polar components of the antibacterial fabric can further promote the formation of the ternary network between the dye-fixing agent and the fibre. However, the surface energy and polar component of the waterproof/breathable fabric are extremely low. It is difficult to maintain the ordered structure of the hydrogen network between the ellagic acid molecule and the dye; therefore, substantial dye loss will occur during washing. The above results further proved that the synergistic effect of the surface properties of functional fabrics and the optimised colour fixation process can influence the water fastness. The stability of dye-fibre interactions under high humidity is governed by moisture-induced swelling and the integrity of the crosslinked network.

5.2 Light fastness performance evaluation

To address the challenges of light fastness faced by the use of natural plant dyes in functional clothing fabrics, this study systematically evaluates the mechanism by which the optimised colour fixation process affects the light fastness of three types of functional fabrics.

In Figure 4, all three fabrics initially achieve a colour fastness rating of 5. 120 h light fastness of antibacterial fabric, the colour fastness of fabric is 3.9 and dye residue rate is 73.6%; 120 h light fastness of UV fabric, the colour fastness of fabric is 3.4 and dye residue rate is 64.1%; 120 h light fastness of waterproof breathable fabric, the colour fastness of fabric is only 2.8 and dye residue rate is 55.3%. The equilibrium structure of

antibacterial fabric is higher, which can promote the formation of a stable molecular network. While the surface energy and polarity of waterproof breathable fabric are extremely low, this will accelerate the decomposition of dye molecules during light exposure. The synergistic effect of the functional fabric's surface properties and the optimised colour fixation process is a key factor in determining light fastness.

Figure 4 Evolution of light fastness performance of three types of functional fabrics (see online version for colours)

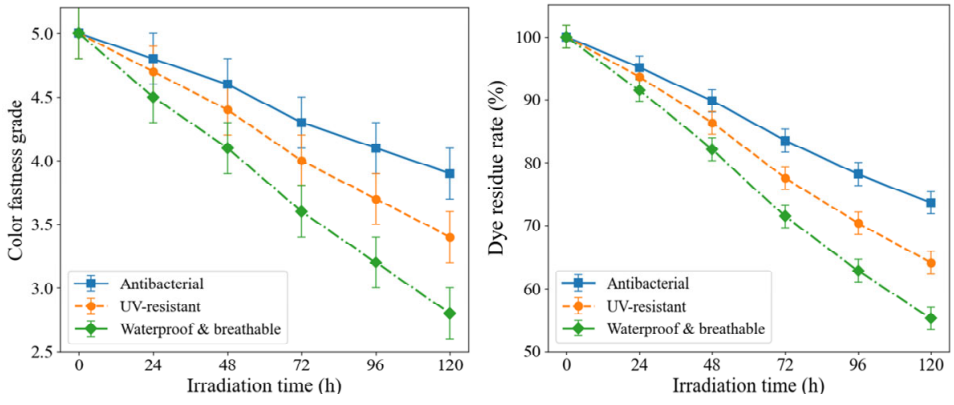

The lightfastness evaluation was conducted at a standard light intensity per ISO 105-B02. The crosslinked network formed by a quaternised chitosan derivative and ellagic acid is expected to confer enhanced light fastness across varying light intensities by reducing the accessibility of oxygen and moisture to dye molecules and by leveraging the UV-absorptive and radical-scavenging properties of ellagic acid.

5.3 Retention of functional fabric properties

To evaluate the influence of the optimised colour fixation process on the original properties of functional fabrics throughout the process, this study examines the retention rates of three typical functional fabric indicators during washing. Antibacterial rate is an important indicator to evaluate the application value of fabric in medical protection and daily hygiene. The ability of fabric to inhibit the growth of bacteria. The fabric's ability to block ultraviolet radiation is an important indicator of the protective effect of outdoor functional clothing's ultraviolet protection factor (UPF). Breathability is the rate at which air permeates the fabric.

As shown in Figure 5, after 25 times of washing, the antibacterial rate of the antimicrobial fabric is still above 91.6%, while the antibacterial rate of the UV-resistant and waterproof/breathable fabric is lower than that. The high surface energy and stable electrostatic adsorption network of the quaternised chitosan derivative are the reasons the antimicrobial fabric retains its original antimicrobial effect. Meanwhile, the UPF retention of UV-resistant fabric is also very excellent. After 25 washes, the UPF value is still 56.5. This is due to the high water contact angle of the UV-resistant fabric and the hydrogen-bond network formed by ellagic acid molecules, which effectively maintains the fabric's original UV protection. In addition, the breathability retention of the waterproof/breathable fabric is the best, reaching 116.7 mm/s after 25 washes. The

microporous structure and the molecular-scale stable network formed by the dye-fixing agent are responsible for this. And the pores of the waterproof/breathable fabric can remain intact after washing. The key performance metrics of the three types of functional fabrics closely match the surface characteristic parameters. It has been proven that dye fastness can be improved by enhancing the dye fixation process. At the same time, the core properties of the three types of functional fabrics can be effectively preserved.

Figure 5 Evolution of the retention of key functional indicators of three types of functional fabrics during washing (see online version for colours)

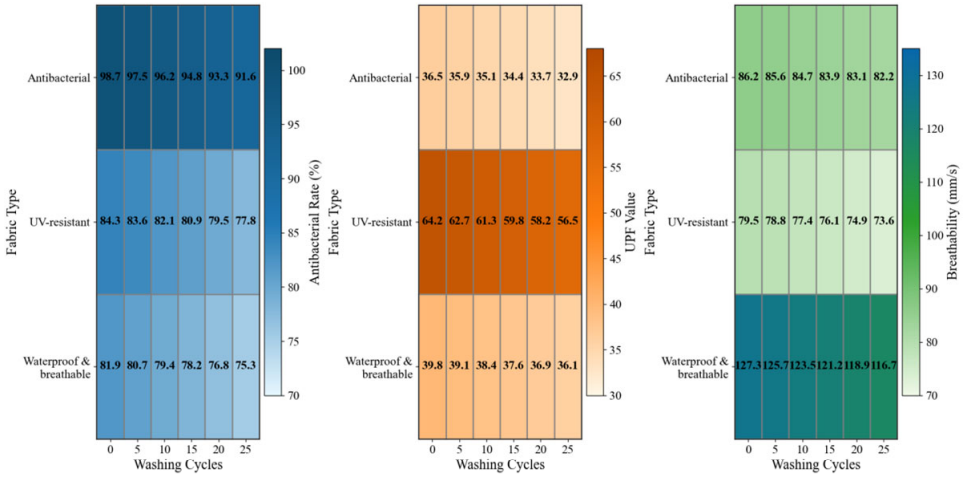

5.4 Fixation process parameter sensitivity

To better understand the effects of fixation process parameters on the colour fastness of natural plant dyes in functional clothing fabrics, this study uses a global sensitivity analysis to determine the contributions of these key process variables. Sobol's first-order index is used as the sensitivity metric; it quantifies the sensitivity of the individual parameter variation to colour fastness and describes the independent effect of a single parameter change on colour fastness. Colour fastness to rubbing is the ability of the fabric's surface to retain dye molecules. It is affected by fibre surface roughness and the degree of molecular crosslinking. By comparing the sensitivity distribution characteristics of five core parameters, temperature, pH, dyeing time, fixing agent concentration, and steam pressure, under the optimised fixation process and the traditional metal mordant dyeing process (referred to as the traditional process), differences in key control parameters for different colour fastness indicators are revealed. Figure 6 shows the sensitivity distributions of various process parameters for water fastness (left sub-plot), light fastness (centre sub-plot), and rubbing fastness (right sub-plot).

In Figure 6, in the water fastness analysis, the Sobol first-order index for pH under the optimised process is 0.34, higher than those for the other parameters, indicating that pH has a decisive influence on the electrostatic bonding strength between the dye and the fibre. This is consistent with the mechanism by which pH modulates the electrostatic interaction energy between the quaternised chitosan derivative and the dye anion during dynamic pH gradient control. In contrast, the pH sensitivity of the conventional process

drops to 0.26, while the steam pressure sensitivity increases to 0.14, reflecting the conventional process's greater reliance on physical parameters.

Figure 6 Sensitivity distribution of fixation process parameters to three colour fastness indicators (see online version for colours)

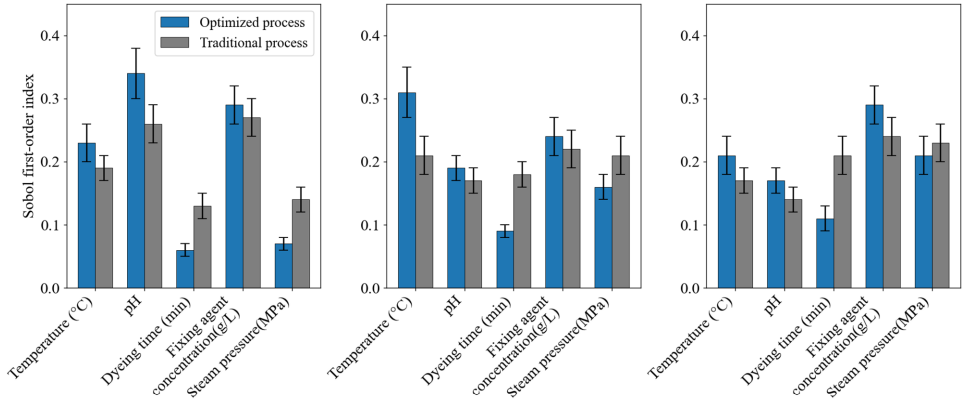

In the lightfastness analysis, the temperature parameter in the optimised process shows the highest sensitivity of 0.31. It is because of the dual effect of temperature on the stability of the dye molecule and the photodegradation reaction. The temperature sensitivity value of the conventional process is 0.21, which shows that the process of conventional technology has no control over the temperature-light stability interaction mechanism.

In the rubbing fastness test, the sensitivity value for the fixing agent concentration in the optimised process is 0.29, which is higher than that of the other parameters, further validating the role of the molecular network formed by the quaternised chitosan derivative and ellagic acid in physical surface adhesion. In the conventional process, the sensitivity of steam pressure is 0.23, which shows that the conventional process technology only depends on the physical pressure to improve the dye attachment.

The optimised process shows more clustered parameter sensitivities across different colour fastness indexes, and sensitivities of different parameters in the optimised process are generally higher than those in the conventional process. It shows that a multi-parameter coupled process model can not only identify the process variables that play a dominant role in different colour fastness, and control them to improve colour fastness, but also systematically improve colour fastness.

5.5 Comparison of the optimised and conventional processes

To further evaluate the effects of natural plant dyes on the optimisation of functional clothing fabrics, this study systematically compares the performance of an optimised colour-fastness process based on quaternised chitosan derivatives and ellagic acid with a conventional metal mordant dyeing process on three types of functional fabrics. The evaluation system covers three dimensions: colour fastness performance (increase in colour fastness to water, light, and rubbing), environmental impact (reduction in wastewater chemical oxygen demand (COD) and heavy metal content), and cost-benefit (change in process time and raw material cost). Colour fastness measures reflect the

stability of the dye in the fabric; environmental measures characterise the eco-friendliness of the process; cost measures quantify economic feasibility. Figure 7 shows the multidimensional improvement rates of the optimised process compared to the traditional process on three types of fabrics: antibacterial fabrics (left sub-figure), UV-resistant fabrics (centre sub-figure), and waterproof and breathable fabrics (right sub-figure).

Figure 7 Multidimensional performance comparison of the optimised fixation process and the traditional metal mordant process on three types of functional fabrics (see online version for colours)

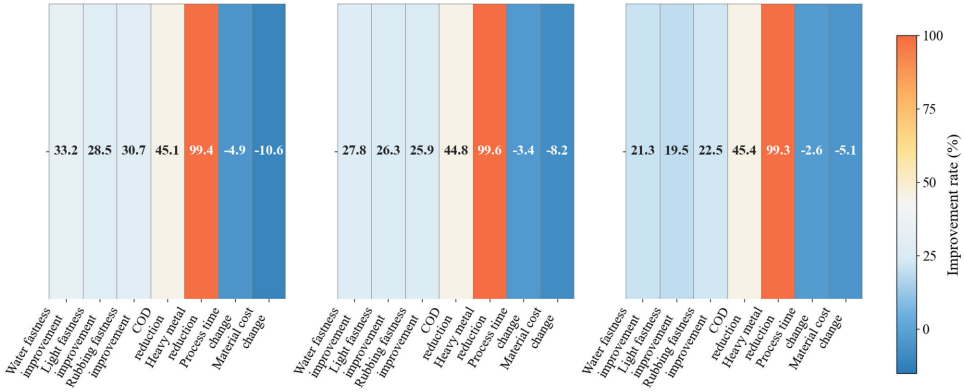

In Figure 7, the optimised process demonstrates the highest colour fastness improvements on the antibacterial fabric, with 33.2% in colour fastness to water, 28.5% in colour fastness to light, and 30.7% in colour fastness to rubbing. This is closely related to the higher surface energy of antibacterial fabrics and the balanced distribution of dispersed and polar components, which are conducive to the formation of a stable electrostatic adsorption network between quaternised chitosan derivatives and dye anions. At the same time, the hydrogen-bond network formed by ellagic acid molecules via eight phenolic hydroxyl groups enhances the dye-fibre binding strength.

In terms of environmental indicators, the heavy metal content of all three fabric types is reduced by over 99%, and the wastewater COD reduction rate remains between 44.8% and 45.4%. This is because the optimised process eliminates the metal mordants chromium and copper used in the conventional process and uses a biocompatible fixing agent system, thereby totally avoiding heavy metal pollution.

Economic analysis shows that the raw material cost reduction rate ranges from –10.6% for antibacterial fabrics to –5.1% for waterproof and breathable fabrics, while the process time change rate ranges from –4.9% to –2.6%. Although the optimised process requires strict control of the dynamic pH gradient and high-temperature steam parameters, the amount of fixing agent is reduced, and the post-process is simplified, thereby decreasing costs.

6 Conclusions

To address the poor colour fastness of natural plant dyes in functional fabrics, the colour fixation process was optimised via multi-parameter coupling, suitable dyes were

screened, and an intermolecular force model was established. Meanwhile, dynamic pH gradient control and high-temperature steam treatment were employed. Finally, a bifunctional colour fixation system composed of a quaternised chitosan derivative and ellagic acid was applied to improve the water fastness, light fastness, and functional stability of the dyeable antibacterial fabric. The water fastness of the dyed antibacterial fabric was improved to level 2.7 after 25 washes, and the dye content was retained at 70.1%. The initial light fastness was level 5, and the light fastness was level 3.9 after 120 hours of exposure. The antibacterial activity was maintained at 91.6% after washes. Both the colour and the function of the antibacterial fabric were well preserved.

Compared with conventional mordant dyeing, the proposed method eliminates heavy-metal pollution by using a metal-free crosslinking system while improving the colour fastness of functional fabrics. In comparison with other documented eco-friendly dyeing processes, this optimised approach demonstrates significant improvements in colour durability and reduced wastewater treatment burden, without compromising the fabrics' inherent functional properties. A preliminary cost assessment suggests that optimised reagent use and simplified post-treatment could improve economic feasibility, particularly by reducing raw material costs and processing time.

Funding

This work was supported by Tangshan University Doctoral Innovation Project BC202432.

Declarations

All authors declare that they have no conflicts of interest.

References

Abdel-Kader, N.S., Abdel-Latif, S.A., El-Ansary, A.L. et al. (2024) 'Design, synthesis, spectroscopic studies, DFT, TD-DFT/PCM calculations, and molecular docking studies on the anti-SARS and anti-COVID-19 activities of novel benzidine bis Azo 1-(2-Hydroxy-3-naphthoic acid) complexes with some transition metal ions', *Polycyclic Aromatic Compounds*, Vol. 44, No. 6, pp.3601–3632.

Aftab, M., Ahmad, T., Adeel, S. et al. (2025) 'Microwave assisted natural dye extraction from Amaltas (Cassia fistula) for cotton dyeing: process optimization using modern statistical and machine learning algorithms', *Natural Product Communications*, Vol. 20, No. 6, pp.1934578X251355408–1934578X251355417.

Alegbe, E.O. and Uthman, T.O. (2024) 'A review of history, properties, classification, applications, and challenges of natural and synthetic dyes', *Heliyon*, Vol. 10, No. 13, pp.e33646–e33664.

Aracena, A., Rezende, M.C. and Pizarro, S. (2024) 'Reproducing the solvatochromism of merocyanines by PCM calculations', *Molecules*, Vol. 29, No. 17, pp.4103–4112.

Bairabathina, V., Shanmugam, K.S.K., Chilukoti, G.R. et al. (2022) 'A review on reverse micellar approach for natural fibre dyeing', *Coloration Technology*, Vol. 138, No. 4, pp.329–341.

Benli, H. (2024) 'Bio-mordants: a review', *Environmental Science and Pollution Research*, Vol. 31, No. 14, pp.20714–20771.

Che, J. and Yang, X. (2022) 'A recent (2009–2021) perspective on sustainable color and textile coloration using natural plant resources', *Heliyon*, Vol. 8, No. 10, pp.e10979–e10993.

Cruz, L., Basílio, N., Mateus, N. et al. (2021) 'Natural and synthetic flavylium-based dyes: the chemistry behind the color', *Chemical Reviews*, Vol. 122, No. 1, pp.1416–1481.

Gala, S., Sumarno, S. and Mahfud, M. (2022) 'Optimization of microwave-assisted extraction of natural dyes from jackfruit wood (Artocarpus heterophyllus Lamk) by response surface methodology', *Engineering and Applied Science Research*, Vol. 49, No. 1, pp.29–35.

Habib, N., Adeel, S., Ali, F. et al. (2021) 'Environmental friendly sustainable application of plant-based mordants for cotton dyeing using Arjun bark-based natural colorant', *Environmental Science and Pollution Research*, Vol. 28, No. 38, pp.54041–54047.

Hannan, M.A., Islam, M.F. and Hoque, M.B. (2023) 'Improvement of mahogany leaf extract dye fixation on cotton-modal blend', *Heliyon*, Vol. 9, No. 10, pp.e20786–e20795.

Harsito, C., Prabowo, A.R., Prasetyo, S.D. et al. (2021) 'Enhancement stability and color fastness of natural dye: a review', *Open Engineering*, Vol. 11, No. 1, pp.548–555.

Hossain, M.A. (2023) 'UV–Visible–NIR camouflage textiles with natural plant based natural dyes on natural fibre against woodland combat background for defence protection', *Scientific Reports*, Vol. 13, No. 1, pp.5021–5037.

Hossain, M.Y., Jiang, T., Zhu, W. et al. (2022) 'Green and sustainable method to improve fixation of a natural functional dye onto cotton fabric using cationic dye-fixing agent/D5 microemulsion', *Journal of Natural Fibres*, Vol. 19, No. 15, pp.11283–11298.

Hosseinnezhad, M., Gharanjig, K., Rouhani, S. et al. (2022) 'Environmentally friendly dyeing of wool yarns using of combination of bio-mordants and natural dyes', *Environmental Progress and Sustainable Energy*, Vol. 41, No. 5, p.e13868.

Hussain, M., Jalali, T., Maftoon-Azad, L. et al. (2024) 'Performance evaluation of natural dye-sensitized solar cells: a comparison of density functional theory and experimental data on chlorophyll, anthocyanin, and cocktail dyes as sensitizers', *ACS Applied Electronic Materials*, Vol. 6, No. 3, pp.1693–1709.

Ibrahim, S.M., Al-Harby, N.F., El-Molla, S.A. et al. (2024) 'New combined experimental and DFT studies for adsorption of sole Azo-dye or binary cationic dyes from aqueous solution', *Scientific Reports*, Vol. 14, No. 1, pp.14756–4773.

Junior, H.L.O., Neves. R.M., Monticeli, F.M. et al. (2022) 'Smart fabric textiles: recent advances and challenges', *Textiles*, Vol. 2, No. 4, pp.582–605.

Lai, C.C. and Chang, C.E. (2021) 'A study on sustainable design for indigo dyeing color in the visual aspect of clothing', *Sustainability*, Vol. 13, No. 7, pp.3686–3696.

Lepre, L.F., Sabelle, S., Beaumard, F. et al. (2021) 'Screening ionic solvents for enhancing the solubility of water-insoluble natural dyes', *Industrial and Engineering Chemistry Research*, Vol. 60, No. 23, pp.8555–8564.

Lin, L., Jiang, T., Xiao, L. et al. (2022) 'Sustainable fashion: eco-friendly dyeing of wool fibre with novel mixtures of biodegradable natural dyes', *Scientific Reports*, Vol. 12, No. 1, pp.21040–21055.

Mandal, S. and Venkatramani, J. (2023) 'A review of plant-based natural dyes in leather application with a special focus on color fastness characteristics', *Environmental Science and Pollution Research*, Vol. 30, No. 17, pp.48769–48777.

Mao, D. and Xu, H. (2024) 'The antimicrobial potential of plant-based natural dyes for textile dyeing: a systematic review using prisma', *AUTEX Research Journal*, Vol. 24, No. 1, pp.20240016–20240040.

Otaviano, B.T.H., Sannomiya, M., de Queiroz, R.S. et al. (2023) 'Natural dye extracted from pomegranate peel: physicochemical characterization, dyeing of cotton fabric, color fastness, and photoprotective properties', *Fibres and Polymers*, Vol. 24, No. 4, pp.1321–1332.

Pizzicato, B., Pacifico, S., Cayuela, D. et al. (2023) 'Advancements in sustainable natural dyes for textile applications: a review', *Molecules*, Vol. 28, No. 16, pp.5954–5975.

Ragab, M.M. and Hassabo, A.G. (2021) 'Various uses of natural plants extracts for functionalization textile based materials', *Journal of Textiles, Coloration and Polymer Science*, Vol. 18, No. 2, pp.143–158.

Saeed, A., Hassan, K. and Sadaf, S.S. (2023) 'A review on colour fastness of natural dyed textiles', *Pakistan Journal of Scientific and Industrial Research Series A: Physical Sciences*, Vol. 66, No. 2, pp.201–212.

Saleem, M.A., Pei, L., Saleem, M.F. et al. (2023) 'Use of quaternary ammonium salt as a dye fixing agent and antimicrobial agent in sustainable, single-step single-bath dyeing and finishing', *Textile Research Journal*, Vol. 93, Nos. 3–4, pp.554–564.

Salian, A., Dutta, S. and Mandal, S. (2021) 'A roadmap to UV-protective natural resources: classification, characteristics, and applications', *Materials Chemistry Frontiers*, Vol. 5, No. 21, pp.7696–7723.

Sk, S., Mia, R., Haque, M.A. et al. (2021) 'Review on extraction and application of natural dyes', *Textile and Leather Review*, Vol. 4, No. 4, pp.218–233.

Talib, A., Adeel, S., Ali, A. et al. (2023) 'Sustainable isolation and application of plant extract-based natural dye for bio-dyeing of silk fabric', *Coatings*, Vol. 13, No. 1, pp.112–121.

Thakker, A.M. and Sun, D. (2021) 'Sustainable plant-based bioactive materials for functional printed textiles', *The Journal of the Textile Institute*, Vol. 112, No. 8, pp.1324–1358.

Turgut, H.I., Elgun, B.S. and Yarar, O. (2023) 'Wash fastness properties of pre-mordanting cotton fabrics dyed with natural dyes', *Journal of Innovative Engineering and Natural Science*, Vol. 4, No. 1, pp.1–17.

Wang, Y., Huang, L., Wang, P. et al. (2024) 'Silk textile finished with natural dyes and UV resistance agents from agricultural waste Aloe Vera rinds', *The Journal of the Textile Institute*, Vol. 115, No. 4, pp.632–638.

Wang, Z., Zhang, Y., Li, N. and Zhang, J. (2026) 'Spatiotemporal patterns and drivers of carbon emissions from on-site wastewater treatment: evidence from a city-wide long-term network', *Environmental Research*, Vol. 296, No. 2026, p.123948.

Xiao, Y.Q. and Kan, C.W. (2022) 'Review on development and application of 3D-printing technology in textile and fashion design', *Coatings*, Vol. 12, No. 2, pp.267–279.